

Direct local observation of magnetic anisotropy in microscopic Ga_{1-x}Mn_xAs dots

M. Malfait,^{a)} K. Vervaeke, J. Fritzsche, and V. V. Moshchalkov
Institute for Nanoscale Physics and Chemistry (INPAC), Nanoscale Superconductivity and Magnetism & Pulsed Fields Group, Katholieke Universiteit Leuven, Celestijnenlaan 200D, Leuven B-3001, Belgium

G. Borghs
IMEC, Kapeldreef 75, 3001 Leuven, Belgium

(Received 23 August 2006; accepted 19 September 2006; published online 6 November 2006)

The effect of the patterning of a Ga_{1-x}Mn_xAs ($x=0.08$) film into an array of microscopic dots on its magnetic properties is locally studied by means of scanning Hall probe microscopy. The measured stray field patterns indicate the presence of a single domain state with a uniform magnetization within the Ga_{1-x}Mn_xAs dots. The magnetic anisotropy of the dot array is directly imaged, revealing a [100] easy axis in the as-grown sample and a $[1\bar{1}0]$ easy axis orientation after annealing. In contrast to a temperature dependent anisotropy in the plain Ga_{1-x}Mn_xAs film, no magnetic easy axis reorientation is observed within the experimentally accessible temperature range. © 2006 American Institute of Physics. [DOI: 10.1063/1.2374859]

The possible application of ferromagnetic semiconductors in electronic devices for spintronics has motivated intense research on Ga_{1-x}Mn_xAs and other diluted magnetic semiconductors (DMSs). When Mn ions are incorporated into GaAs, they introduce magnetic moments but also act as acceptors, providing holes that mediate the ferromagnetic interaction between the localized Mn spins. Ferromagnetism in Ga_{1-x}Mn_xAs films can only be obtained at a Mn content x which is far above the equilibrium solubility limit of Mn in GaAs.¹ Therefore nonequilibrium growth conditions must be applied, which can be realized using molecular beam epitaxy (MBE) with growth temperatures in the range of 200–300 °C. These low growth temperatures inevitably lead to a high density of As antisite and Mn interstitial (Mn_i) defects,² which compensate a fraction of the holes generated by the substitutional Mn ions^{3–5} thus reducing the ferromagnetic coupling in the Ga_{1-x}Mn_xAs layer. It has recently been shown that the amount of Mn_i defects can be reduced significantly by annealing at low temperatures (even below the growth temperature),² as the highly mobile Mn_i ions diffuse towards the surface⁶ where they are passivated through oxidation⁷ or, if an As capping layer is present, by forming MnAs.⁸ This mechanism explains the large increase in the Curie temperature T_C and the conductivity upon annealing which was previously observed.^{9,10}

Ga_{1-x}Mn_xAs exhibits a well defined and quite strong magnetic anisotropy, which shows rich characteristics such as in-plane/out-of-plane anisotropy,¹¹ superimposed with a cubic anisotropy combined with an in-plane uniaxial anisotropy.¹² Moreover, the anisotropy depends on the epitaxial strain, as well as on the Mn content, the hole density, and temperature.^{13,14} This can lead to large changes in the anisotropy upon annealing or to temperature induced reorientations of the easy axis.^{15–17} Both the in-plane/out-of-plane anisotropy and the cubic anisotropy are well understood within the framework of the mean field p - d Zener model of the hole-mediated ferromagnetism in which the spin-orbit

coupling in the valence band is taken into account.^{13,14} Although the origin of the in-plane uniaxial contribution is still under debate, Sawicki *et al.* have recently shown that a small trigonal distortion is sufficient to describe the uniaxial anisotropy and its dependence on the hole concentration and temperature, in terms of the same p - d Zener model.¹⁵

The magnetic behavior of DMS at small length scales is an important issue for the possible application of these materials in microelectronics. In this letter we study the effect of the patterning of a Ga_{1-x}Mn_xAs film into an array of microscopic dots on its magnetic properties. As the reduced size of these dots requires local measuring techniques, we used scanning Hall probe microscopy (SHPM) as a noninvasive tool to directly image the magnetic configuration and anisotropy of the Ga_{1-x}Mn_xAs dots.

A Ga_{1-x}Mn_xAs film with Mn content $x=0.08$ was grown by low-temperature molecular beam epitaxy: First a 100 nm high-temperature GaAs buffer layer was deposited under standard conditions on a semi-insulating epi-ready (001) GaAs substrate, followed by a low-temperature (LT) GaAs buffer of the same thickness. Subsequently the Ga_{1-x}Mn_xAs layer was grown with a nearly stoichiometric As₂ flux at a temperature ≈ 15 °C below the Mn segregation limit, which was established during a preceding test deposition. The growth was monitored *in situ* by reflection high energy electron diffraction, which showed a clear (1×2) reconstruction. The high structural quality and the sample thickness of 98 nm were confirmed with x-ray diffraction measurements. After the growth a part of the wafer was subjected to a post-growth annealing treatment in an oxygen atmosphere⁷ for about 175 h at 185 °C. The Curie temperature was determined with superconducting quantum interference device (SQUID) magnetometry from the temperature dependence of the magnetization, as the onset of the ferromagnetic order. For the as-grown sample $T_C=53$ K, while after the post-growth annealing treatment the Curie temperature has increased up to $T_C=140$ K.

Magnetic hysteresis measurements with the field applied along the four main in-plane crystallographic orientations re-

^{a)}Electronic mail: mathieu.malfait@fys.kuleuven.be

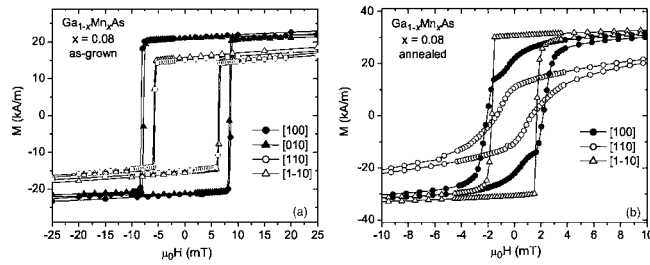


FIG. 1. Magnetic field dependence of the magnetization of a plain (a) as-grown and (b) annealed $\text{Ga}_{1-x}\text{Mn}_x\text{As}$ ($x=0.08$) films measured at 5 K for different sample orientations with respect to the applied magnetic field. In graph (b) the curve along the [010] axis is omitted for clarity, as it is similar to that along the [100] axis.

veal a complex magnetic anisotropy of both the as-grown and the annealed $\text{Ga}_{1-x}\text{Mn}_x\text{As}$ ($x=0.08$) layer. As can be seen from Fig. 1(a), a biaxial anisotropy with easy axes along the [100] and [010] crystallographic directions is observed at $T=5$ K for the as-grown layer, while after annealing [see Fig. 1(b)] the magnetic anisotropy is uniaxial with a $[1\bar{1}0]$ easy axis at 5 K. In both cases a reorientation transition of the easy axis is observed at higher temperatures (not shown). In the as-grown $\text{Ga}_{1-x}\text{Mn}_x\text{As}$ ($x=0.08$) layer the anisotropy changes to a uniaxial anisotropy with $[1\bar{1}0]$ easy axis at temperatures $T > 30$ K. In the annealed sample the anisotropy is uniaxial over the entire temperature range, but a temperature induced reorientation transition of the easy axis from $[1\bar{1}0]$ to $[110]$ is observed when the temperature is increased above $T \approx 90$ K.¹⁸

A part of the wafer was patterned by means of photolithography. For this purpose the sample surface was covered with positive photoresist (JSR micro-PFR 7790G) and a resist pattern was applied that consists of a square array of disks each having a diameter of $4 \mu\text{m}$ with a period of $12 \mu\text{m}$. The sample was then immersed for 2 min in a 1:1:50 $\text{H}_3\text{PO}_4:\text{H}_2\text{O}_2:\text{H}_2\text{O}$ phosphoric acid solution to chemically etch the uncovered parts of the film. Due to a strong underetch of the highly doped $\text{Ga}_{1-x}\text{Mn}_x\text{As}$ layer, rounded dots were formed rather than thin cylinders, as can be seen from Fig. 2 which shows the atomic force microscopy (AFM) image of a single dot. The AFM image reveals a total etch depth of roughly 130 nm and a dot diameter of $3.4 \mu\text{m}$. The image also indicates that the strong underetch is related to the high Mn content, since the underetch is much smaller for the last 30 nm above the substrate, i.e., in the LT-GaAs buffer layer. Figure 3(a) shows an optical image of the resulting array of $\text{Ga}_{1-x}\text{Mn}_x\text{As}$ dots. An adjacent part of the

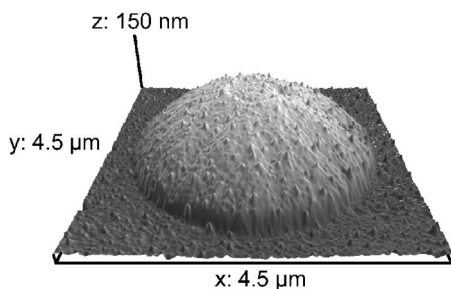


FIG. 2. AFM image of a microscopic $\text{Ga}_{1-x}\text{Mn}_x\text{As}$ ($x=0.08$) dot. The dots were obtained through photolithography and chemical etching in a phosphoric acid solution.

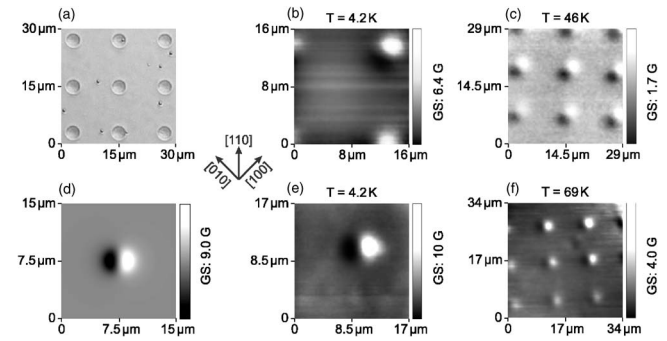


FIG. 3. (a) Optical image of an array of microscopic $\text{Ga}_{1-x}\text{Mn}_x\text{As}$ dots. [(b) and (c)] Magnetic image of a dot array obtained from an as-grown $\text{Ga}_{1-x}\text{Mn}_x\text{As}$ layer at (b) 4.2 K and (c) 46 K. [(e) and (f)] Magnetic image of a dot array etched from an annealed $\text{Ga}_{1-x}\text{Mn}_x\text{As}$ layer at (e) 4.2 K and (f) 69 K. (d) z component of the stray field of a sphere segment with uniform magnetization, simulated with the finite-element method. The gray scale (GS) bar at the right of every magnetic image indicates the amplitude of the stray fields. The orientation axes apply to each image.

wafer was subjected to the postgrowth annealing treatment described above, before it was subjected to the same etching procedure.

By means of a commercial scanning Hall probe microscope the magnetic stray fields of the microscopic $\text{Ga}_{1-x}\text{Mn}_x\text{As}$ dots were directly imaged. The experimental setup consists of a SHPM device which is inserted into a temperature-controlled liquid helium cryostat. The magnetic field probe consists of a submicron Hall cross which is patterned by the use of e-beam lithography in a MBE-grown GaAs/AlGaAs heterostructure with a two-dimensional electron gas. This Hall probe was scanned over the sample to measure the surface magnetic fields at a height of $0.85 \mu\text{m}$ above the sample surface. The scan range reaches up to $19 \mu\text{m}$ at 4.2 K and increases with temperature up to $150 \mu\text{m}$ at room temperature.

Figures 3(b) and 3(c) show the SHPM image of the as-grown $\text{Ga}_{1-x}\text{Mn}_x\text{As}$ ($x=0.08$) dot array at 4.2 and 46 K, respectively. An array of magnetic dipoles is observed with the same periodicity as the $\text{Ga}_{1-x}\text{Mn}_x\text{As}$ dots, which clearly indicates that these dipoles result from the spontaneous in-plane magnetization of $\text{Ga}_{1-x}\text{Mn}_x\text{As}$, and that the dots are in a uniformly magnetized state. Every magnetic dipole points in the [100] direction which is therefore confirmed to be a magnetic easy axis. The fact that all dipoles point along the same axis and have the same orientation although no external field was intentionally applied can be attributed to a remanent field in the superconducting magnet of the cryostat or even to the earth magnetic field which may align the magnetic moments of the $\text{Ga}_{1-x}\text{Mn}_x\text{As}$ disks as they are cooled through the Curie temperature. Note that in conventional ferromagnets such as Co or Permalloy a similar single domain state is only observed at much smaller dimensions.^{19,20} Due to shape anisotropy larger dots typically show a flux closing configuration, the so-called vortex state, which reduces their magnetostatic energy and leads to a stray field pattern that is quite different from that observed in Fig. 3.²¹ Macroscopically large magnetic domains with uniform magnetization on the scale of hundreds of micrometers have been directly observed in $\text{Ga}_{1-x}\text{Mn}_x\text{As}$ films by means of magneto-optical imaging²² and scanning Hall probe microscopy.²³ Moreover, since the shape anisotropy field is typically an order of magnitude smaller than the magnetocrystalline anisotropy in

$\text{Ga}_{1-x}\text{Mn}_x\text{As}$, the direction of the magnetization is determined by the magnetocrystalline rather than by the shape anisotropy. The magnetization in a $\text{Ga}_{1-x}\text{Mn}_x\text{As}$ dot with a diameter of $3.4\ \mu\text{m}$ may therefore indeed be uniform as indicated by the observed stray field pattern.

In contrast to the plain $\text{Ga}_{1-x}\text{Mn}_x\text{As}$ ($x=0.08$) layer, the easy axis does not change to the $[1\bar{1}0]$ orientation when the temperature is increased above 30 K [see Fig. 3(c)]. This different anisotropy behavior could be the result of small variations of the composition of the $\text{Ga}_{1-x}\text{Mn}_x\text{As}$ layer, but it might as well be attributed to the increase in surface to volume ratio by a factor of ≈ 2 of the etched dot with respect to the plain film. This relative surface increase can affect the strain relaxation in the $\text{Ga}_{1-x}\text{Mn}_x\text{As}$ and may also lead to a slight reduction in the hole density due to the Fermi level pinning at the surface. A strong dependence of the magnetic anisotropy on both the lattice strain and the charge carrier density is a well established property of $\text{Ga}_{1-x}\text{Mn}_x\text{As}$.^{13,14}

The magnetic anisotropy of the $\text{Ga}_{1-x}\text{Mn}_x\text{As}$ dot array could not be studied by SQUID magnetometry, as the small magnetic signal, due to the low remaining $\text{Ga}_{1-x}\text{Mn}_x\text{As}$ volume of the etched samples, could not be resolved from the diamagnetic background of the substrate and the sample holder.

The magnetic images of the annealed $\text{Ga}_{1-x}\text{Mn}_x\text{As}$ ($x=0.08$) dots measured at $T=4.2\ \text{K}$ and $T=69\ \text{K}$ are shown in Figs. 3(e) and 3(f), respectively. From these images it is clear that the low temperature magnetic easy axis is rotated by 45° upon annealing and now resides along the $[1\bar{1}0]$ direction. The easy axis reorientation transition which is expected around 90 K could not be studied as the magnetic signal was too low to be resolved from the elevated thermal noise from the Hall probe in this temperature range. The stray field of a rounded dot with uniform magnetization along the $[1\bar{1}0]$ direction was simulated using the finite-element method, where the dot was modeled as a sphere segment with a height of 98 nm and a sphere radius of $15.2\ \mu\text{m}$, in correspondence to AFM measurements, and with a magnetization of 32 kA/m, in agreement with the SQUID magnetization data of the annealed $\text{Ga}_{1-x}\text{Mn}_x\text{As}$ ($x=0.08$) layer. These simulations confirm the dipolelike stray field pattern, as shown in Fig. 3(d), which shows the z component of the calculated stray field at a height of 850 nm above the substrate. The magnitude of the simulated stray field shows a good correspondence to that of the stray field measured with SHPM. The slightly larger stray field pattern that is experimentally observed can be attributed to the finite size of the active region of the Hall cross ($\sim 0.5 \times 0.5\ \mu\text{m}^2$), which leads to a somewhat convoluted, and thus larger, image. The correspondence to the experimental stray field pattern corroborates a single domain state of the $\text{Ga}_{1-x}\text{Mn}_x\text{As}$ dots.

In summary, arrays of microscopic magnetic dots were fabricated from both an as-grown and an annealed $\text{Ga}_{1-x}\text{Mn}_x\text{As}$ ($x=0.08$) film, which, due to a strong underetch in the $\text{Ga}_{1-x}\text{Mn}_x\text{As}$ layer, have a rounded shape. By means of

scanning Hall probe microscopy the magnetic anisotropy of the dot array was directly imaged, revealing a $[100]$ easy axis in the as-grown sample and a $[1\bar{1}0]$ orientation of the easy axis after annealing. Microscopic patterning may affect the $\text{Ga}_{1-x}\text{Mn}_x\text{As}$ anisotropy behavior to some extent, since, in contrast to the plain $\text{Ga}_{1-x}\text{Mn}_x\text{As}$ film, no temperature induced reorientations of the magnetic easy axis were observed. The measured stray field patterns indicate a single domain state with a uniform magnetization within the microscopic $\text{Ga}_{1-x}\text{Mn}_x\text{As}$ dots and can be reproduced by finite-element method simulations.

The authors are thankful to M. J. Van Bael for the help with the SQUID magnetometer. This work was supported by the Fund for Scientific Research-Flanders (Belgium) (F.W. O.-Vlaanderen), the K. U. Leuven Research Fund GOA/2004/2 program, and the Belgian IUAP.

¹H. Ohno, A. Shen, F. Matsukura, A. Oiwa, A. Endo, S. Katsumoto, and Y. Iye, *Appl. Phys. Lett.* **69**, 363 (1996).

²K. M. Yu, W. Walukiewicz, T. Wojtowicz, I. Kuryliszyn, X. Liu, Y. Sasaki, and J. K. Furdyna, *Phys. Rev. B* **65**, 201303 (2002).

³S. Sanvito, G. Theurich, and N. Hill, *J. Supercond.* **15**, 85 (2002).

⁴F. Máca and J. Mašek, *Phys. Rev. B* **65**, 235209 (2002).

⁵S. C. Erwin and A. G. Petukhov, *Phys. Rev. Lett.* **89**, 227201 (2002).

⁶K. W. Edmonds, P. Boguslawski, K. Y. Wang, R. P. Campion, S. N. Novikov, N. R. S. Farley, B. L. Gallagher, C. T. Foxon, M. Sawicki, T. Dietl, M. Buongiorno Nardelli, and J. Bernholc, *Phys. Rev. Lett.* **92**, 037201 (2004).

⁷M. Malfait, J. Vanacken, W. Van Roy, G. Borghs, and V. V. Moshchalkov, *Appl. Phys. Lett.* **86**, 132501 (2005).

⁸M. Adell, L. Ilver, J. Kanski, V. Stanciu, P. Svedlindh, J. Sadowski, J. Z. Domagala, F. Terki, C. Hernandez, and S. Charar, *Appl. Phys. Lett.* **86**, 112501 (2005).

⁹T. Hayashi, Y. Hashimoto, S. Katsumoto, and Y. Iye, *Appl. Phys. Lett.* **78**, 1691 (2001).

¹⁰S. J. Potashnik, K. C. Ku, S. H. Chun, J. J. Berry, N. Samarth, and P. Schiffer, *Appl. Phys. Lett.* **79**, 1495 (2001).

¹¹F. Matsukura, M. Sawicki, T. Dietl, D. Chiba, and H. Ohno, *Physica E (Amsterdam)* **21**, 1032 (2004).

¹²For a review, see M. Sawicki, *Acta Phys. Pol. A* **106**, 119 (2004), and references therein.

¹³T. Dietl, H. Ohno, F. Matsukura, J. Cibert, and D. Ferrand, *Science* **287**, 1019 (2000).

¹⁴T. Dietl, H. Ohno, and F. Matsukura, *Phys. Rev. B* **63**, 195205 (2001).

¹⁵M. Sawicki, K.-Y. Wang, K. W. Edmonds, R. P. Campion, C. R. Staddon, N. R. S. Farley, C. T. Foxon, E. Papis, E. Kamińska, A. Piotrowska, T. Dietl, and B. L. Gallagher, *Phys. Rev. B* **71**, 121302 (2005).

¹⁶V. Stanciu and P. Svedlindh, *Appl. Phys. Lett.* **87**, 242509 (2005).

¹⁷K.-Y. Wang, M. Sawicki, K. W. Edmonds, R. P. Campion, S. Maat, C. T. Foxon, B. L. Gallagher, and T. Dietl, *Phys. Rev. Lett.* **95**, 217204 (2005).

¹⁸M. Malfait (unpublished).

¹⁹O. Kazakova, M. Hanson, P. Blomquist, and R. Wäppling, *J. Appl. Phys.* **90**, 2440 (2001).

²⁰R. P. Cowburn, D. K. Koltsov, A. O. Adeyeye, M. E. Welland, and D. M. Tricker, *Phys. Rev. Lett.* **83**, 1042 (1999).

²¹T. Shinjo, T. Okuno, R. Hassdorf, K. Shiget, and T. Ono, *Science* **289**, 930 (2000).

²²U. Welp, V. K. Vlasko-Vlasov, X. Liu, J. K. Furdyna, and T. Wojtowicz, *Phys. Rev. Lett.* **90**, 167206 (2003).

²³A. Pross, S. Bending, K. Edmonds, R. P. Campion, C. T. Foxon, and B. L. Gallagher, *J. Appl. Phys.* **95**, 3225 (2004).